Testing General Relativity with the Reflection Spectrum of the Supermassive Black Hole in 1H0707-495

Zheng Cao,[1] Sourabh Nampalliwar,[1,2] Cosimo Bambi,[1,2,*] Thomas Dauser,[3] and Javier A. García[4,3,5]
[1]*Center for Field Theory and Particle Physics and Department of Physics, Fudan University, 200433 Shanghai, China*
[2]*Theoretical Astrophysics, Eberhard-Karls Universität Tübingen, 72076 Tübingen, Germany*
[3]*Remeis Observatory and ECAP, Universität Erlangen-Nürnberg, 96049 Bamberg, Germany*
[4]*Cahill Center for Astronomy and Astrophysics, California Institute of Technology, Pasadena, California 91125, USA*
[5]*Harvard-Smithsonian Center for Astrophysics, Cambridge, Massachusetts 02138, USA*

(Received 30 August 2017; revised manuscript received 12 January 2018; published 1 February 2018)

Recently, we have extended the x-ray reflection model RELXILL to test the spacetime metric in the strong gravitational field of astrophysical black holes. In the present Letter, we employ this extended model to analyze *XMM-Newton*, *NuSTAR*, and *Swift* data of the supermassive black hole in 1H0707-495 and test deviations from a Kerr metric parametrized by the Johannsen deformation parameter α_{13}. Our results are consistent with the hypothesis that the spacetime metric around the black hole in 1H0707-495 is described by the Kerr solution.

DOI: 10.1103/PhysRevLett.120.051101

In four-dimensional general relativity, the no-hair theorem guarantees that the only stationary and asymptotically flat vacuum black hole solution, which is regular on and outside the event horizon, is the Kerr metric [1]. It is also remarkable that the spacetime around astrophysical black holes formed by complete gravitational collapse in the Universe should be well approximated by the Kerr geometry [2]. Nevertheless, general relativity has been mainly tested in weak gravitational fields, in particular, with Solar System experiments and radio observations of binary pulsars [3]. The strong gravity regime is largely unexplored, and there are a number of scenarios beyond Einstein's gravity that provide the same predictions for weak fields and present differences when gravity becomes strong.

The study of the properties of the electromagnetic radiation emitted by the gas in the accretion disk can potentially probe the spacetime metric around astrophysical black holes and test the Kerr nature of these objects [4]. Previous work has shown that x-ray reflection spectroscopy (the so-called iron line method) [5] is a promising technique to do this job [6]. Currently, the most advanced x-ray reflection model to describe the spectrum from the strong gravity region of a Kerr black hole is RELXILL [7]. In Ref. [8], we have described RELXILL_NK, an extension of RELXILL to non-Kerr spacetimes (here NK stands for non-Kerr), and we have shown with some simulations how this new model can test the nature of astrophysical black holes. In this Letter, we employ RELXILL_NK for the first time to analyze real data and constrain possible deviations from the Kerr solution.

Let us first briefly review the physics and astrophysics behind x-ray reflection spectroscopy. Within the disk-corona model [9], an accreting black hole is surrounded by a geometrically thin and optically thick disk. The corona is a hotter cloud near the black hole. For instance, it might be the base of the jet, the atmosphere above the inner part of the disk, or some accreting material between the disk and the black hole. Its geometry is currently unknown. Because of inverse Compton scattering of thermal photons from the disk off free electrons in the corona, the latter becomes an x-ray source with a power-law spectrum. The corona also illuminates the disk, producing a reflection component with some fluorescent emission features, the most prominent of which is usually the iron $K\alpha$ line, which is at 6.4 keV in the case of neutral and weakly ionized iron and shifts up to 6.97 keV for H-like iron ions. Due to gravitational redshift, Doppler boosting, and light bending, the reflection spectrum is detected in the flat faraway region with a shape different from that at the emission point and encodes all the details about the strong gravity region near the black hole [4].

There are two natural approaches to test the Kerr black hole hypothesis [2]. In the so-called top-down approach, we consider a specific alternative theory of gravity in which black holes are not described by the Kerr metric and we check whether astrophysical data prefer the Kerr or non-Kerr metric. There are two problems to following this method. First, there are a large number of alternative theories of gravity, and none seems to be more motivated than others, so we should repeat the analysis for every theory. Second, rotating black hole solutions in alternative theories of gravity are known only in quite exceptional cases, while the nonrotating or slow-rotating solutions are not very useful to test astrophysical black holes because the spin plays an important role in the shape of the spectrum.

In the bottom-up approach, we employ a phenomenological test metric in which possible deviations from the Kerr solution are quantified by one or more "deformation

parameters." The Kerr metric is recovered when all the deformation parameters vanish, and we want to check whether astrophysical data require vanishing deformation parameters, that is, if astrophysical black holes are indeed the Kerr black holes as expected in Einstein's gravity. There are several such phenomenological metrics available in literature today [4]. It is important to note that these metrics are not always obtained from some alternative theories of gravity. As such, these metrics and their deformation parameters do not have a well motivated background. Their significance instead lies in the fact that they capture deviations from a Kerr metric.

In this Letter, as an explorative study, we follow this bottom-up approach and we employ the Johannsen metric with the deformation parameter α_{13} [10] (see also the Supplemental Material for the line element and the physical interpretation [11]). The Kerr metric is recovered when $\alpha_{13} = 0$. In order to have a regular exterior region (no singularities or closed timelike curves), we have to impose the following restriction to the value of α_{13} [10]

$$\alpha_{13} \geq -\left(1 + \sqrt{1 - a_*^2}\right)^3, \tag{1}$$

where a_* is the dimensionless spin parameter. We choose to perform the analysis with α_{13} here as an illustration of the capabilities of this model for testing non-Kerr metrics. Further studies, involving both α_{13} and α_{22} and other astrophysical sources, are underway.

The supermassive black hole in the Narrow Line Seyfert 1 galaxy 1H0707-495 looks to be a quite promising source for testing the Kerr metric using x-ray reflection spectroscopy. Its spectrum has significant edge features, which are commonly interpreted as an extremely strong reflection component. Previous studies that assumed the Kerr metric and a reflection dominated spectrum found the inner edge of the accretion disk very close to the black hole (thus increasing the relativistic effects in the spectrum), a moderate inclination angle, and an extremely high iron abundance [12–15]. Note that some authors suggest that the spectrum is instead dominated by a powerful wind. This is clear in IRAS13224 [16], and it may be possible in 1H0707-495 as well [17]. In this Letter, we have focused on the most popular reflection model [12–15], because our main motivation is to test the new model rather than to determine which is the correct model for this source, but the wind model is also an important scenario and it should be investigated in a more detailed study.

XMM-Newton, *NuSTAR*, and *Swift* observations of 1H0707-495 are shown in Table I. In our study, for *XMM-Newton*, we have only considered the observation in 2011: it corresponds to the lowest flux state ever observed possessing clear edge features. For the same reason, the 2011 observation has been investigated by several authors, which is helpful for the choice of the models and the comparison of the results. The three separated observations of *NuSTAR* in 2014 have simultaneous snapshots of *Swift*. However, the second *Swift* observation was taken during an anomaly period of this mission and therefore was not included in our analysis. A brief description of the data reduction is reported in the Supplemental Material [11].

TABLE I. Observations of 1H0707-495. In this Letter, we have only considered the *XMM-Newton* observation of 2011, the three *NuSTAR* observations, and the first and the third *Swift* observations.

Mission	Obs. ID	Year	Exposure (ks)
XMM-Newton	0511580101	2008	124
	0511580201	2008	124
	0511580301	2008	123
	0511580401	2008	122
	0653510301	2010	117
	0653510401	2010	128
	0653510501	2010	128
	0653510601	2010	129
	0554710801	2011	98
NuSTAR	60001102002	2014	144
	60001102004	2014	49
	60001102006	2014	47
Swift	00080720001	2014	20
	00080720003	2014	17
	00080720004	2014	17

We have performed three separated studies (named analysis 1, 2, and 3) employing the following models, respectively,

$$\begin{aligned} &\text{Model 1}: \ \text{TBABS} * (\text{RELXILL\_NK} + \text{DISKBB}), \\ &\text{Model 2}: \ \text{TBABS} * (\text{RELXILL\_NK} + \text{RELXILL\_NK}), \\ &\text{Model 3}: \ \text{TBABS} * \text{RELXILL\_NK}. \end{aligned} \tag{2}$$

Our results are summarized in Table II and in Figs. 1 and 2. The reflection spectrum of the disk in the Johannsen metric is described by RELXILL_NK, in which the free parameters are the black hole spin a_*, the deformation parameter α_{13}, the inclination angle of the disk i, the emissivity index q assuming a simple power-law $1/r^q$, where r is the radial coordinate, the photon index of the primary component from the corona Γ, the ionization of the disk $\log \xi$, and the iron abundance $A_{\rm Fe}$ (in solar units). TBABS takes the galactic dust absorption into account and the column number density has been set to the value measured for 1H0707-495 ($N_{\rm H} = 5.8 \times 10^{20}$ cm^{-2}) [15].

In analysis 1, we have fitted the *XMM-Newton* EPIC-pn data with model 1. We have employed DISKBB to fit the "soft excess" around 1 keV as done in Ref. [13]. The corresponding constraint on the spin and the deformation parameters are shown in the left panel of Fig. 1, where the red, green, and blue lines indicate, respectively, the 68%, 90%, and 99% confidence level curves.

TABLE II. Summary of the best-fit values. The row data indicate which observations have been used. The row Model indicates the Xspec model employed, and the number refers to that in Eq. (2). The reported uncertainty corresponds to the 90% confidence level. In analysis 3, we have used the Cash statistics instead of the χ^2 one. See the text for more details.

	Analysis 1	Analysis 2	Analysis 3	
Data	*XMM-Newton* 2011	*XMM-Newton* 2011	*NuSTAR* +*Swift*	
Model	1	2	3	
a_*	$0.96^{+0.01}_{-0.08}$	>0.98	>0.99	RELXILL_NK
α_{13}	$-0.8^{+1.4}_{-0.7}$	$-0.05^{+0.1}_{-1.0}$	$-0.6^{+0.6}_{-0.2}$	
i (deg)	38^{+4}_{-7}	49^{+2}_{-2}	41^{+2}_{-3}	
q	$3.6^{+1.1}_{-0.4}$	$3.9^{+0.5}_{-0.5}$	$3.7^{+0.1}_{-0.1}$	
Γ	$1.33^{+0.07}_{-0.10}$	$2.49^{+0.03}_{-0.02}$	$3.29^{+0.02}_{-0.01}$	
			$2.59^{+0.04}_{-0.02}$	
			$3.13^{+0.06}_{-0.01}$	
$\log \xi$	<1.79	$1.29^{+0.02}_{-0.05}$	$2.15^{+0.24}_{-0.07}$	
$A_{\rm Fe}$	>8.6	>9.3	>9.6	
$T_{\rm in}$	0.150 ± 0.003			DISKBB
$\log \xi'$		$3.30^{+0.01}_{-0.06}$		RELXILL_NK
$A_{\rm Fe}{}'$		>9.6		
χ^2/d.o.f.	$127/94 = 1.35$	$157/94 = 1.67$	1938/3246 (C-stat/d.o.f.)	

In analysis 2, we have fitted the same *XMM-Newton* data with model 2 following what was done with a Kerr metric in Refs. [13,15]. The double reflection model is one of the most popular models to fit the soft excess in active galactic nuclei like 1H0707-495 in which the soft spectrum changes significantly with the flux state. There are a few physical scenarios to motivate a double reflection model, but the basic idea is that there are certain inhomogeneities in the accretion disk. For instance, the density of the disk photosphere may be patchy, leading to mixed regions of high and low ionization [18]; the surface of the disk may have regions of different density [13]; it is possible that we are looking at a disk with different layers [15]. The parameters of the two reflection models are tied with the exception of the ionization, iron abundance, and normalization. The corresponding constraints on a_* and α_{13} are shown in the right panel in Fig. 1.

The minimum of the reduced χ^2 is not very close to 1 for analysis 1 and analysis 2. This is because the *XMM-Newton* data have a very high signal to noise ratio below 1.5 keV and any model that cannot perfectly fit the soft excess has a relatively large reduced χ^2 (see Ref. [19] for a discussion on this point). The residuals between 1 and 4 keV might be due, for example, to a highly ionized outflowing wind [14]. We could obtain a reduced χ^2 closer to 1 excluding data below 1 or 1.5 keV, as done in some of previous studies in the literature [19]. Note, however, that the difficulty to fit the soft energy band is not crucial in the present study, for which the goal is to test the Kerr metric and constrain on the deformation parameter α_{13}, because our results are mainly sensitive to the iron $K\alpha$ complex, which is at higher energies. Note that the fit is driven by the small error bars from the soft energy band.

Finally, in analysis 3, we have fitted the *NuSTAR* and *Swift* data with model 3 following the study in the Kerr metric in Ref. [15]. We impose that the values of the model parameters are the same for the three observations, with the exception of the photon index Γ, as done in [15] (in analyses 1 and 2, we have only one photon index because we only consider the observation of 2011). Note that, in analysis 3, we have used the Cash statistics because of low photon count. The constraints on a_* and α_{13} are shown in Fig. 2; they are better than those from *XMM-Newton*, but it is not easy to identify the main reason, as the observations are different (source at different times, different exposure times, different energy range of the data, etc.).

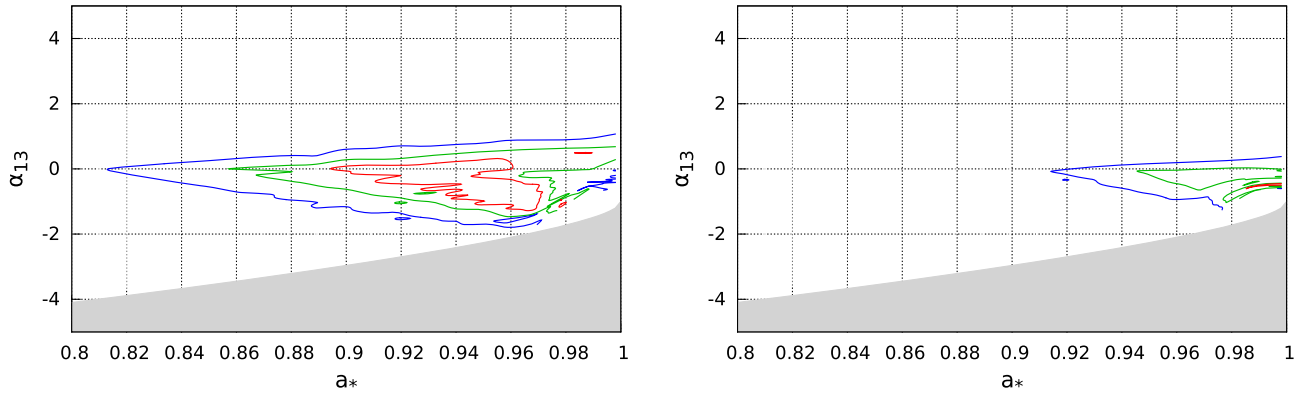

FIG. 1. Constraints on the spin parameter a_* and the Johannsen deformation parameter α_{13} from the *XMM-Newton* data of 2011: analysis 1 (left) and analysis 2 (right). The red, green, and blue lines indicate, respectively, the 68%, 90%, and 99% confidence level curves for two relevant parameters. The grayed region is ignored in our study because it does not meet the condition in Eq. (1). See the text for more details.

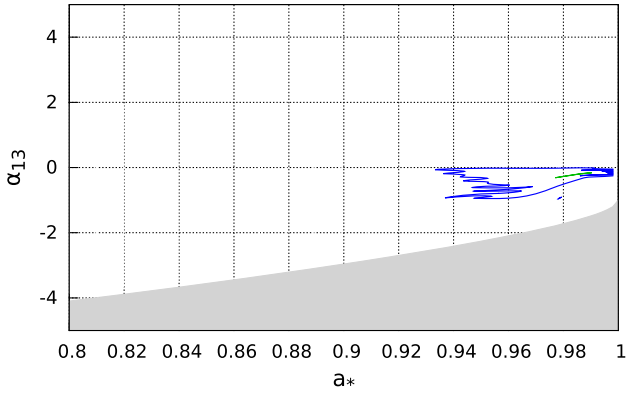

FIG. 2. As in Fig. 1 from analysis 3 (*NuSTAR+Swift*). The 68% confidence level curve is too thin to be plotted. See the text for more details.

In Ref. [8], generic simulations were performed to test the capabilities of RELXILL_NK in analyzing observations from present and future instruments. We found that *LAD/eXTP* [20] can provide significantly stronger constraints on α_{13} than *NuSTAR*. Here we consider the specific case of 1H0707-495 and hypothetical future observations with X-IFU/Athena [21]. For model 1, which is less constrained, a 300 ks observation can distinguish a spacetime with $\alpha_{13} = -0.5$ from Kerr solutions at 99% confidence level (see Supplemental Material for more details [11]). Thus, 1H0707-495 with a best-fit α_{13} of -0.8, if observed with X-IFU/Athena for 100 ks, will be clearly distinguishable from a Kerr black hole. On the other hand, if $\alpha_{13} = 0.5$, it is not possible to exclude Kerr and $\alpha_{13} = -1$ even with an observation of 300 ks. The constraint on α_{13} strongly depends on the black hole spin. An extended study of the constraining power of present and future x-ray missions will be presented in a future paper.

Conclusions.— In this Letter, we have employed for the first time a new version of RELXILL designed to test the Kerr nature of astrophysical black holes to analyze *XMM-Newton*, *NuSTAR*, and *Swift* data of the supermassive black hole in 1H0707-495. We have chosen this source because the spectrum has a very strong iron $K\alpha$ line and the inner edge of the accretion disk extends up to very small radii. Assuming that the spectrum is reflection dominated, our results are summarized in Table II and in Figs. 1 and 2, and are consistent with the assumption that the metric around the supermassive black hole in 1H0707-495 is described by the Kerr solution, as expected in general relativity. Work is currently underway to study other black holes with RELXILL_NK as well as to constrain other deformation parameters or to test black hole metrics from specific gravity theories.

Z. C. thanks the Cahill Center for Astronomy and Astrophysics at Caltech for hospitality during his visit where part of this work was done. The work of Z. C., S. N., and C. B. was supported by the National Natural Science Foundation of China (Grant No. U1531117) and Fudan University (Grant No. IDH1512060). C. B. and J. A. G. acknowledge support from the Alexander von Humboldt Foundation.

*Corresponding author.
bambi@fudan.edu.cn

[1] B. Carter, Phys. Rev. Lett. **26**, 331 (1971); D. C. Robinson, Phys. Rev. Lett. **34**, 905 (1975); P. T. Chrusciel, J. L. Costa, and M. Heusler, Living Rev. Relativity **15**, 7 (2012).
[2] C. Bambi, *Black Holes: A Laboratory for Testing Strong Gravity* (Springer, Singapore, 2017).
[3] C. M. Will, Living Rev. Relativity **17**, 4 (2014).
[4] C. Bambi, Rev. Mod. Phys. **89**, 025001 (2017).
[5] A. C. Fabian, K. Iwasawa, C. S. Reynolds, and A. J. Young, Publ. Astron. Soc. Pac. **112**, 1145 (2000); L. W. Brenneman and C. S. Reynolds, Astrophys. J. **652**, 1028 (2006); C. S. Reynolds, Space Sci. Rev. **183**, 277 (2014).
[6] J. Schee and Z. Stuchlik, Gen. Relativ. Gravit. **41**, 1795 (2009); T. Johannsen and D. Psaltis, Astrophys. J. **773**, 57 (2013); C. Bambi, Phys. Rev. D **87**, 023007 (2013); J. Jiang, C. Bambi, and J. F. Steiner, Astrophys. J. **811**, 130 (2015); C. Bambi, J. Jiang, and J. F. Steiner, Classical Quantum Gravity **33**, 064001 (2016); J. K. Hoormann, B. Beheshtipour, and H. Krawczynski, Phys. Rev. D **93**, 044020 (2016); M. Zhou, A. Cardenas-Avendano, C. Bambi, B. Kleihaus, and J. Kunz, Phys. Rev. D **94**, 024036 (2016); Y. Ni, M. Zhou, A. Cardenas-Avendano, C. Bambi, C. A. R. Herdeiro, and E. Radu, J. Cosmol. Astropart. Phys. 07 (**2016**) 049; C. Bambi, Z. Cao, and L. Modesto, Phys. Rev. D **95**, 064006 (2017).
[7] T. Dauser, J. Garcia, J. Wilms, M. Bock, L. W. Brenneman, M. Falanga, K. Fukumura, and C. S. Reynolds, Mon. Not. R. Astron. Soc. **430**, 1694 (2013); J. Garcia, T. Dauser, C. S. Reynolds, T. R. Kallman, J. E. McClintock, J. Wilms, and W. Eikmann, Astrophys. J. **768**, 146 (2013); J. Garcia *et al.*, Astrophys. J. **782**, 76 (2014).
[8] C. Bambi, A. Cardenas-Avendano, T. Dauser, J. A. Garcia, and S. Nampalliwar, Astrophys. J. **842**, 76 (2017).
[9] G. Matt, G. C. Perola, and L. Piro, Astron. Astrophys. **247**, 25 (1991); A. Martocchia and G. Matt, Mon. Not. R. Astron. Soc. **282**, L53 (1996).
[10] T. Johannsen, Phys. Rev. D **88**, 044002 (2013).
[11] See Supplemental Material at http://link.aps.org/supplemental/10.1103/PhysRevLett.120.051101 for more details on the line element employed, the data analysis and reduction, a discussion on the systematic effects, and some simulations with a future X-ray mission.
[12] A. C. Fabian *et al.*, Nature (London) **459**, 540 (2009); A. Zoghbi, A. Fabian, P. Uttley, G. Miniutti, L. Gallo, C. Reynolds, J. Miller, and G. Ponti, Mon. Not. R. Astron. Soc. **401**, 2419 (2010).
[13] A. C. Fabian *et al.*, Mon. Not. R. Astron. Soc. **419**, 116 (2012).
[14] T. Dauser, J. Svoboda, N. Schartel, J. Wilms, M. Dovčiak, M. Ehle, V. Karas, M. Santos-Lleó, and H. L. Marshall, Mon. Not. R. Astron. Soc. **422**, 1914 (2012).
[15] E. Kara *et al.*, Mon. Not. R. Astron. Soc. **449**, 234 (2015).
[16] M. L. Parker *et al.*, Nature (London) **543**, 83 (2017).

[17] K. Hagino, H. Odaka, C. Done, R. Tomaru, S. Watanabe, and T. Takahashi, Mon. Not. R. Astron. Soc. **461**, 3954 (2016); M. L. Parker *et al.* (unpublished).
[18] A. M. Lohfink, C. S. Reynolds, J. M. Miller, L. W. Brenneman, R. F. Mushotzky, M. A. Nowak, and A. C. Fabian, Astrophys. J. **758**, 67 (2012).
[19] D. R. Wilkins, E. Kara, A. C. Fabian, and L. C. Gallo, Mon. Not. R. Astron. Soc. **443**, 2746 (2014).
[20] S. N. Zhang *et al.* (eXTP Collaboration), Proc. SPIE Int. Soc. Opt. Eng. **9905**, 99051Q (2016).
[21] http://www.the-athena-x-ray-observatory.eu/.